Available online at www.sciencedirect.com
ScienceDirect
Polymer 48 (2007) 165–173
polymer
www.elsevier.com/locate/polymer

Poly[bis(2-aminophenyloxy)disulfide]: A polyaniline derivative containing disulfide bonds as a cathode material for lithium battery

Yu-Zhi Su [a,*], Wen Dong [a], Jian-Hua Zhang [a], Jian-Hua Song [a], Yong-Hua Zhang [b], Ke-Cheng Gong [b]

[a] *Department of Chemistry, School of Chemistry and Chemical Engineering, Guangzhou University, Guangzhou 510006, Guangdong, China*
[b] *Polymer Structure and Modification Research Laboratory, South China University of Technology, Guangzhou 510641, China*

Received 27 April 2006; received in revised form 3 October 2006; accepted 22 October 2006
Available online 29 November 2006

Abstract

A new conductive polyaniline derivative containing disulfide bonds, poly[bis(2-aminophenyloxy)disulfide] (PAPOD), has been proposed as a high energy-storage material. PAPOD has been synthesized using a moderate oxidant ferric chloride and characterized by elemental analysis, X-ray photoelectron spectroscopy (XPS), FT-IR, FT-Raman, and UV–vis spectroscopy. The cyclic voltammograms of this polymer show that the intramolecular self-catalysis occurs between the conductive main-chain polyaniline (doping/undoping processes of the π-conjugated system) and side-chain disulfide bonds (scission/reformation processes of the S–S bonds) in PAPOD. Because the redox reaction of conductive main-chain polyaniline occurs in the same potential range as that of the side-chain disulfide bonds of this polymer, the Li/PAPOD test cell displays a charge capacity of 230 mAh g^{-1}-cathode and an energy density of 460 mWh g^{-1}-cathode, which is about 2–3 times higher than those of inorganic intercalation compounds.

Keywords: Poly[bis(2-aminophenyloxy)disulfide]; Conducting polymer; Organodisulfide

1. Introduction

The development of a lightweight and high energy-density rechargeable battery is of comparative importance because of the increasing demand for mobile power with the extensive use of portable devices. The energy density of nowadays lithium or lithium-ion battery is mainly restricted by lower charge density of the cathode materials, e. g., 100–150 mAh g^{-1} for inorganic intercalation compounds such as $LiCoO_2$, $LiMn_2O_4$, or $LiNiO_2$. Based on the reversible polymerization–depolymerization process ($RS-SR + 2e^- = 2RS^-$), disulfide compounds have been first proposed by Visco et al. [1] as the candidates for high energy-density organic/polymeric cathode materials in lithium batteries. Among them, 2,5-dimercapto-1,3,4-thiadiazole (DMcT) is regarded as one of the most well known organodisulfur compounds due to its high theoretical charge density, high potential vs lithium, and high stability to cycling and temperature [2].

Oyama and co-workers [3,4] reported a new composite cathode materials composed of DMcT and polyaniline (PANi) in which the redox reaction rate of disulfide bonds was accelerated due to the electrocatalysis effect of PANi on the disulfide bonds. PANi is well known as a conductive and electroactive polymer. But it does not have sufficient energy density for practical application as a cathode material to a rechargeable battery. It is usually believed that PANi functions not only as the molecular current collector and active cathode material but also as a catalyst to the redox reaction of organodisulfides in the composite cathode such as DMcT/PANi [5–8]. Despite the attractive advantage of these PANi/organodisulfides composite

* Corresponding author.
E-mail address: subox@163.net (Y.-Z. Su).

0032-3861/$ - see front matter © 2006 Elsevier Ltd. All rights reserved.
doi:10.1016/j.polymer.2006.10.044

cathodes, these composite cathodes have some unfavorable properties for battery application, namely, a relatively low current capability, poor solubility in typical organic solvent such as propylene carbonate (PC) during the reduction process, and slow redox at room temperature owing to the limited catalysis of PANi to the redox of disulfide bonds based on macroscopic mixing neither microscopic nor intermolecular merging between PANi and organodisulfides in these composite materials.

In order to solve these problems, very recently, two new types of polymers containing disulfide bonds have been proposed. In the first type of these compounds, the disulfide bonds can be bound into the backbone chain of a polymer [9–13]. These polymers are not soluble in organic electrolytes during the reduction process. However, the capacities of these polymers decrease. This disadvantage of these materials may be caused by cleavage of the main chain containing disulfide bonds and the difficulty in re-production of disulfide bonds due to their steric hindrance [14]. In the second type of these compounds, the disulfide bonds can be linked to the side chain of a conducting polymer [15–20]. These polymers have three advantages in comparison with the conventional orgnosulfur compounds. First, these polymers have rather high electric conductivity; second, the cleavage and recombination of disulfide bonds may be facile as the materials have the confined polymer configuration which is interconnected with disulfide bonds; third, the catalysis efficiency can be improved owing to the fact that the electrocatalysis of the conducting main-chain to side chain S–S bonds may take place in the intramolecular or microscopic range in these conducting polymers [21–23].

In this paper, a new conductive polyaniline derivative containing disulfide bond, poly[bis(2-aminophenyloxy)disulfide] (PAPOD), has been proposed as a novel energy-storage material. The synthesis of PAPOD using chemical oxidation and its characterization by elemental analysis, X-ray photoelectron spectroscopy (XPS), FT-IR, FT-Raman, and UV–vis spectroscopy have been reported. The electrical properties, electrochemical behavior, and discharge/charge performance of this new conducting polymer have also been investigated.

2. Experimental section

2.1. Materials

o-Aminophenol, triethylamine, sulfur monochloride and ferric chloride were of reagent grade and were purchased from Shanghai Reagent Company. *o*-Aminophenol was recrystallized from methanol. Aniline, acetonitrile (AN), dimethyl formamide (DMF) and tetrahydrofuran (THF) were distilled twice under reduced pressure before use. Lithium perchlorate (Aldrich) was dried at 150 °C for 2 h to remove the absorbed water. Battery-grate propylene carbonate (PC) (analytic grade, Fluka), ethylene carbonate (EC) (analytic grade, Fluka), and lithium foil with approximately 250 μm thickness (Lithco co., Ltd.) were stored under an inert atmosphere. All other chemicals (reagent grade) were purchased from Guangzhou Chemical Plant and used as received.

2.2. Measurements

Proton NMR spectrum was recorded on a Bruker DRX-400 spectrometer. Deuterated $CDCl_3$ was used as a solvent and tetramethylsilane (TMS) as the internal standard. Fourier transform infrared (FT-IR) and Fourier transform Raman spectra (FT-Raman) were performed on a Nicolet 5DX with KBr plates and a Nicolet 950 instrument, respectively. Elemental analysis was measured on a Vario EL elemental analytical instrument. X-ray photoelectron spectroscopy (XPS) measurements were carried out by using a VG ESCA/SIMS LAB MKV spectrometer with an Al Kα X-ray source. The vacuum-dried sample was mounted on a standard VG sample holder by double side Scotch tape. All core-level spectra are referenced to the hydrocarbon component in the C_{1s} envelope defined to be 285.0 eV to compensate for surface charging.

The thermogravimetric analysis (TGA) was determined on a Perkin–Elmer TGA-2 with a heating rate of 2 °C min^{-1} under N_2. DC conductivity measurement was performed using pressed pellets of PAPOD powder under pressure (~100 MPa) by utilizing a 4-probe technique at room temperature.

Cyclic voltammetry was carried out using a standard three-electrode, two-compartment electrochemical cell employing an EG&G PAR Model 273 potentiostat/galvanostat with an Ag/AgCl (sat. KCl) electrode as the reference electrode, a platinum strip coated with PAPOD polymer or its monomer as the working electrode, and a blank platinum strip as the counter electrode. The cyclic voltammograms were recorded on a 3086 *x–y* recorder at room temperature. The working electrode, PAPOD or its momoner coated on a platinum strip, was prepared by casting from saturated DMF solutions. All solutions were deaerated for 10 min with argon before measurements and a gas flow was maintained upon the solution throughout the experiments.

2.3. Synthesis of APOD

Scheme 1 shows the synthetic procedure for monomer bis(2-aminophenyloxy)disulfide (APOD). *o*-Aminophenol 21.8 g (0.2 mol) along with 10.1 g (0.1 mol) triethylamine was dissolved in 300 mL dichloromethane. To this well stirred solution at 0–3 °C was added 20.0 g (ca. 0.15 mol) of sulfur monochloride diluted with 100 mL of dichloromethane at a rate regulated to keep the temperature in the 0–3 °C range. Addition usually required approximately 1 h, after that the reaction was stirred for another 30 min. All the reaction was run under argon atmosphere. Amine hydrochloride was removed from the

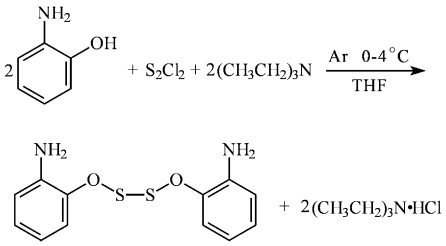

Scheme 1.

solution by filtering and dichloromethane was removed under reduced pressure using a rotating evaporator. After recrystallization two times from a mixture of ether and methanol (1:1, v/v) at low temperature, the crystals were dried in a vacuum at room temperature for 24 h, and then stored in a refrigerator prior to use. Yield of the product was 38%. The decomposition temperature of it is 83–85 °C. ^{1}H NMR (500 MHz, $CDCl_3$) δ: 6.74 (4H, dd, ArH), 1.88 (2H, d, NH). FT-IR (KBr): 3374, 3303, 3050, 1595, 1503, 1468, 1405, 1271, 1215, 1145, 1032, 899, 765 cm^{-1}. FT-Raman: 3380, 3308, 3072, 1594, 1516, 1474, 1381, 1281, 1206, 1157, 1036, 769, 574 cm^{-1}. Elem Anal: Calcd for $C_{12}H_{12}O_2N_2S_2$: C, 51.41; H, 4.32; N, 9.99; S, 22.87. Found: C, 49.97; H, 4.78; N, 10.28; S, 23.98.

2.4. Synthesis of PAPOD

PAPOD was synthesized according to the method of Diaz et al. [24–27]. APOD 1.4 g (5 mmol) was placed in a vacuum-dried Morton flask and cooled down in an ice-water bath. After evacuating and flushing with argon for three times, $FeCl_3$ 2.0 g (12.5 mmol) and 2.0 M HCl 15.0 mL (30 mmol) dissolved in AN 15.0 mL (kept in ice-water bath) were then added dropwise to the above solution with stirring. The mixture was stirred in argon atmosphere at 0–3 °C for 6 h. During this time, the slurring became dark blue-black. The mixture was filtered and washed with CH_3CN. The residue was extracted continuously (Soxhlet) with CH_3CN until the extract was clear (24 h) and then dried overnight under vacuum at ambient temperature to obtain 0.87 g of PAPOD.

2.5. HCl-doping and undoping of PAPOD

PAPOD 0.2 g was suspended in 1.0 M aqueous HCl 20 mL, stirred vigorously for 4 h. The product was filtered, washed with deionized water, and then dried in a vacuum oven for 48 h. A fine dark blue powder of HCl-doped PAPOD was obtained. The undoped PAPOD was obtained by keeping PAPOD in aqueous NH_4OH (1:1) solution and stirring for 6 h. The mixture was filtered, washed simultaneously with NH_4OH (1:1) solution. The product was dried at vacuum for 48 h, and a dark tan powder was obtained. Elem Anal: Found for HCl-doped PAPOD: C, 40.12; H, 2.86; N, 7.86; S, 19.36. Found for undoped PAPOD: C, 51.06; H, 2.83; N, 9.04; S, 24.16.

3. Results and discussion

3.1. Characterization of the polymer

3.1.1. X-ray photoelectron spectroscopy (XPS)

XPS spectra of the C_{1s}, N_{1s}, O_{1s}, and S_{2p} regions of HCl-doped PAPOD are shown in Fig. 1. All the spectra were recorded under the identical condition. The decomposition of C_{1s} peak gives four peaks as shown in Fig. 1a. The first one, also the most intense one, which is situated at 284.8 eV, is attributed to C–C or C–H bonds. The second one situated at 286.3 eV can be assigned to the C–N or C=N bonds. Both of them have a fwhm (full width at half-maximum) of 1.7 eV. The third one situated at 287.1 eV and the fourth one at 288.3 eV, which have a fwhm of 2.9 eV, can be referred to the $C{=}N^+$ or $C{-}N^+$ bonds and the C–O or C=O bonds, respectively [12,16,28].

The N_{1s} spectrum can be deconvoluted into four peaks as shown in Fig. 1b. The first contribution situated at 398.3 eV and the second contribution at 399.3 eV can be assigned to the imine group (–N=) and amine group (–NH–), respectively [29,30]. The identities of the other two high binding energy components at 400.2 and 401.4 eV are still controversial among the researchers. They have been attributed to the charged-N sites in variable valence field of the counterions [31], protonated imine- and amine-N [32,33], or polaronic and bipolaronic [34]. However, the total area of both of these components is well related to the amount of counteranions intercalated [28,32,33] and hence the N-doping level – the fraction of protonated N sites in the polymer – can be evaluated such that the HCl-doping level of PAPOD is 39%. In contrast to the doping level of HCl-doping PANi (ca. 50%), the doping level of PAPOD is lower than that of HCl-doped PANi, which indicates that the relatively lower conductivity of PAPOD would be presented as is discussed later.

The O_{1s} envelope (Fig. 1c) can be deconvoluted into three compounds, corresponding to three different chemical environments which have been assigned as C=O (531.0 eV), C–O or C–S (532.0 eV), and H_2O (533.2 eV) [12,28,30]. The S_{2p} envelope (Fig. 1d) contains two components, corresponding to two different chemical environments ($S_{2p1/2}$ and $S_{2p3/2}$). The first one situated at 166.9 eV can be attributed to sulfur covalently bonded to the oxygen, while the second, situated at 171.1 eV should be attributed to S=O bonds [12,16]. These results confirmed that the –O–S–S–O– bonds are found in PAPOD.

3.1.2. Ultraviolet–visible spectroscopy

The electronic spectra of the undoped and HCl-doped PAPOD dissolved in DMF are compared in Fig. 2. The spectrum of undoped state (Fig. 2a) is characterized by two electronic transitions at about 310 and 551 nm, respectively. The electronic transition at shorter wavelength is assigned to the π–π^* transition of benzenoid ring on the basis of earlier studies on polyaniline [35] and is related to the extent of conjugation between adjacent phenyl rings in polymer chain. The transition at longer wavelength is due to the "exciton" transition caused by the interchain or intrachain charge transfer [36]. This band has been found to be dependent on the overall oxidation state of the polymer [37,38]. Moreover, the intensity of the transition at 310 nm is significantly higher in comparison with the transition at 551 nm, while in the case of the unsubstituted PANi the two transitions have approximately the same intensity [39,40]. This is probably due to the lower quinoneimine content of PAPOD related to PANi. This result is in excellent agreement with that of XPS above as well as FT-IR below, in which the lower quinoid ($\sim$1621 cm^{-1}) to benzenoid ($\sim$1517 cm^{-1}) band intensity ratio is observed.

Both 310 and 551 nm bonds undergo a hypsochromic shift compared with conventional PANi and sulfonated PANi [41–43]. The hypsochromic shift suggests that the steric effect

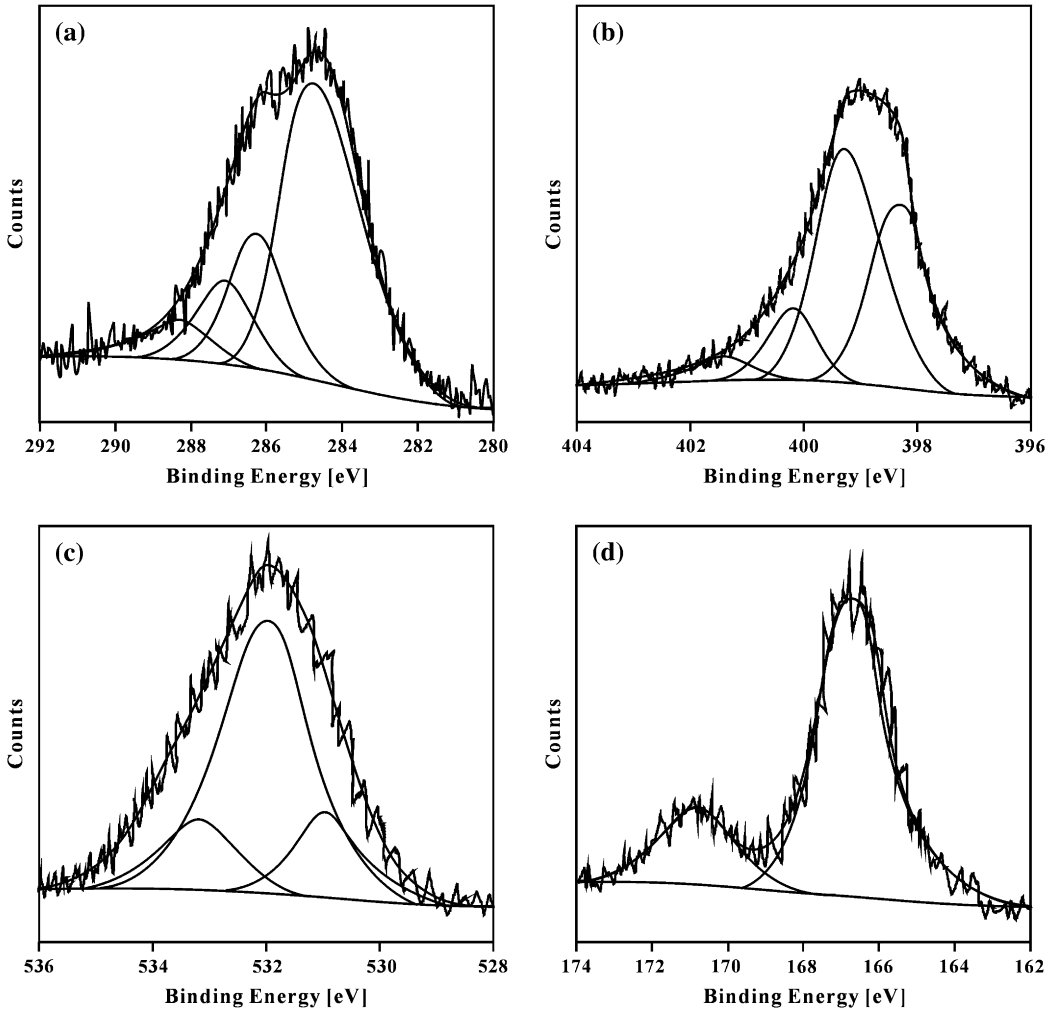

Fig. 1. XPS spectra of HCl-doped PAPOD: (a) C_{1s}, (b) N_{1s}, (c) O_{1s}, and (d) S_{2p}.

of the −O−S−S−O− groups in the polymer chain causes perturbation in the coplanarity of the π system, hence lowering the degree of conjugation as well as hindering charge transfer between the chains. The bond gap increases which led to the observed decrease in conductivity. This result is consistent with that reported for sulfonic ring-substituted PANi [35–37].

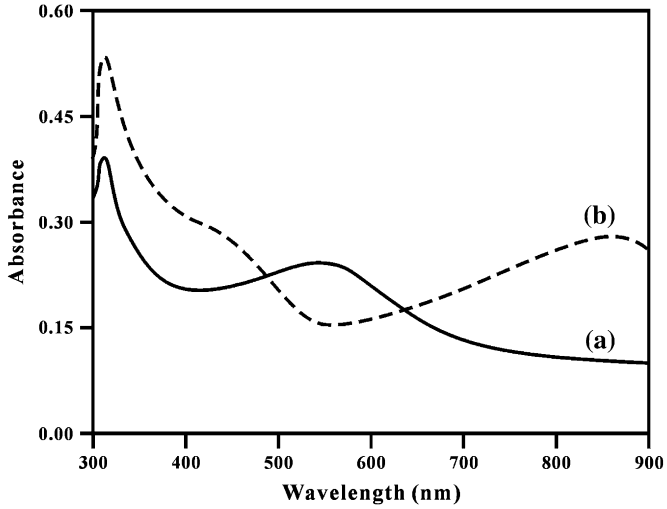

Fig. 2. UV–vis spectra of the (a) undoped and (b) HCl-doped PAPOD in DMF.

When the PAPOD is doped with HCl, a dramatic change in electronic spectrum is observed. The spectrum is shown in Fig. 2b. Doping with HCl does not alter the position of the peak at about 310 nm related to the *p*-phenylenediamine units, but the band at about 551 nm completely disappears and two new bands are observed at 426 and 865 nm, which are assigned to the formation of polarons (radical cations) from quinoneimine units on the polymer chains.

3.1.3. Fourier transform infrared and Raman spectroscopy (FT-IR and FT-Raman)

The FT-IR spectra of the undoped and HCl-doped PAPOD are given in Fig. 3. The number of peaks and their positions are essentially the same in both spectra while some of their relative intensities vary much. In Fig. 3a the band at 1621 cm^{-1} is assigned to the C=N and C=C stretching of the quinoid diimine units and the band at 1517 cm^{-1} to the C=C stretching of benzenoid diamine units [25]. The small band at 1309 cm^{-1} is attributed to the quinoid group, while the band at about 1252 cm^{-1} can be attributed to the imine group C=N

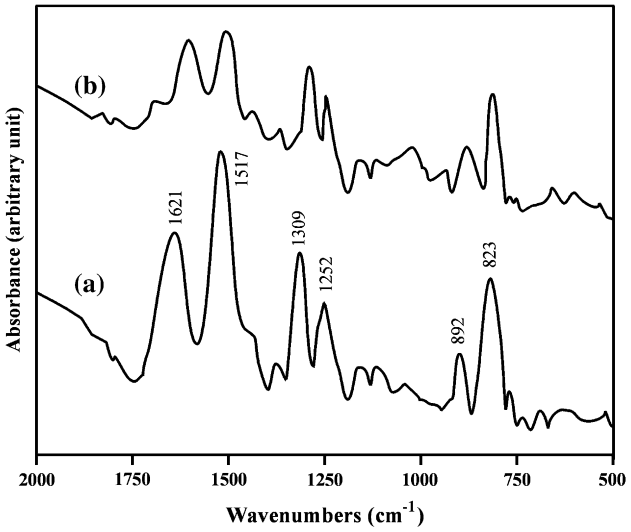

Fig. 3. FT-IR spectra of (a) undoped and (b) HCl-doped PAPOD.

[44,45]. The absorption peak at about 892 and 823 cm^{-1} should be attributed to γ_{C-H} of 1,2,4-substituted aromatic ring [46], which demonstrates that a coupling occurs in the *para* position with respect to the NH_2 group. The ratio between the intensities of these two bands is a measure of the oxidation degree of the polymer. The band ratio of A_{1517}/A_{1621} is 1.4–1.5 and the band ratio of A_{1517}/A_{1621} of the unsubstituted undoped PANi is 1.0–1.1. It is estimated that PAPOD contains only one quinoneimine unit after approximately four benzenoid monomeric units while PANi contains only one quinoneimine unit after three benzenoid monomeric units. The proposed configuration of undoped PAPOD is shown in Scheme 2 and compared with the structure of PANi in Scheme 3.

As PAPOD is converted to HCl-doped PAPOD, the quinoneimine band at 1621 cm^{-1} and the benzene-ring band at

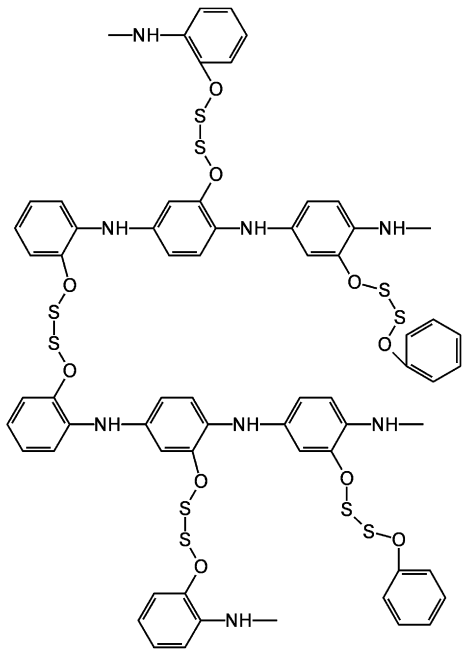

Scheme 2.

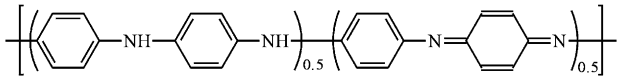

Scheme 3.

1517 cm^{-1} in neutral state shift to lower frequencies at 1602 and 1504 cm^{-1}, respectively, in acid state. Shifting of these bands after protonation or doping is very well known in the case of unsubstituted PANi and other substituted PANi [29,39,47].

The FT-Raman spectra of neutral and acid state PAPOD are shown in Fig. 4. The number of peaks and their positions are nearly the same in both the spectra of Figs. 3 and 4. However, some of their relative intensities vary remarkably. The strong band at 1003 and 565 cm^{-1} is attributed to the stretching vibrations of the C–C and S–S bands, respectively, which are very weak in corresponding FT-IR.

3.2. Properties of the polymer

3.2.1. Electrical conductivity

Electrical conductivity measurement has been done on the pellet sample of PAPOD. The pellet was made by pressing PAPOD powders and the contact was made by silver sheet. The electrical conductivity of PAPOD is 6.4×10^{-2} S cm^{-1} at room temperature, being 2–3 orders of magnitude smaller than that of HCl-doped compressed PANi pellet. The origin of lower conductivity might be caused by the steric effect of the specific structure of PAPOD. The bridge group –O–S–S–O– substituent between *ortho* positions of PANi can be expected to induce an additional ring twisting along the polymer backbone due to the increased steric hindrance. Such induced ring twisting not only increases the energy barrier for charge transport but can also reduces the extent of polaron delocalization along the chain [29,48]. However, the electrical conductivity of PAPOD is rather high in comparison with that of the conventional organosulfur compounds, which exhibit no

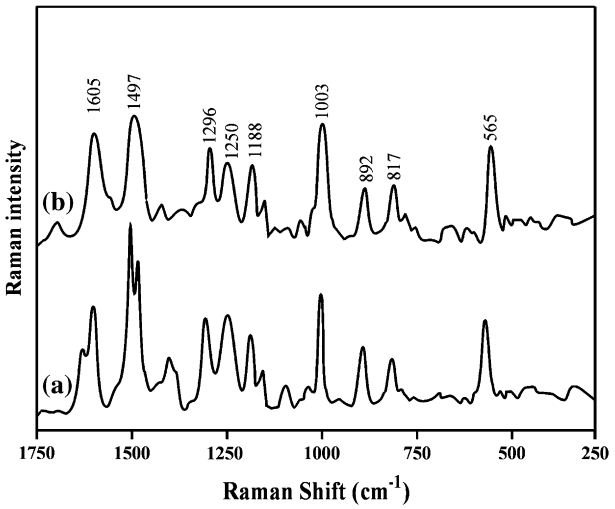

Fig. 4. FT-Raman spectra of (a) undoped and (b) HCl-doped PAPOD.

electrical conductivity. This conducting organodisulfide polymer is of great advantage for the energy-storage materials such as the cathode material.

It is widely believed that a key control factor for obtaining high conductivity polymer is the pH of acidified media. The pH dependence of conductivity for HCl-doped solid measured by four-probe method under ambient temperature is shown in Fig. 5. The pH value is identified as the HCl concentration of AN solution containing 0.1 mol dm^{-3} APOD monomer. It is clear that the conductivity of PAPOD decreases by more than six orders of magnitude in the region of pH = 0–3. In fact, the polymerization efficiency as well as the electroactivity of polymer shows striking enhancement and the electrical conductivity of polymer increases with the growth in acid content of the solution.

3.2.2. Redox properties

Kinetic reversibility is an important parameter for energy-storage material. The higher the kinetic reversibility of the redox reaction is, the higher the power output is at a given energy efficiency of the system or the higher the energy efficiency is at a given power output. The kinetic reversibility of the redox couples can be assessed according to the separation of the anodic and cathodic peak potentials in cyclic voltammogram.

The cyclic voltammogram of monomer APOD film adhered on a platinum foil in 0.1 mol dm^{-3} $LiClO_4$/AN solution is shown in Fig. 6a. In the first sweep of the potential from 0 to 0.8 V, no oxidative peaks are observed, which indicates that no oxidative reaction has occurred initially between the potential range of 0–0.8 V. One reduction peak at −0.54 V is observed when the potential is reversed from 0.8 to −0.8 V. This cathode peak can be assigned to the reduction of S–S bonds in APOD. However, one oxidation peak at 0.38 V is also observed when the potential is swept from a negative potential to a positive potential again. This anode peak corresponds to oxidative of the thiolate, which is formed at the reduction, to form the S–S bonds.

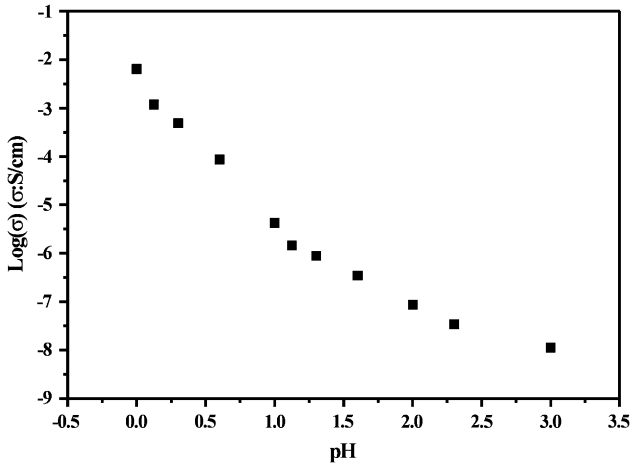

Fig. 5. pH dependence of DC conductivity at room temperature for HCl-doped PAPOD solid.

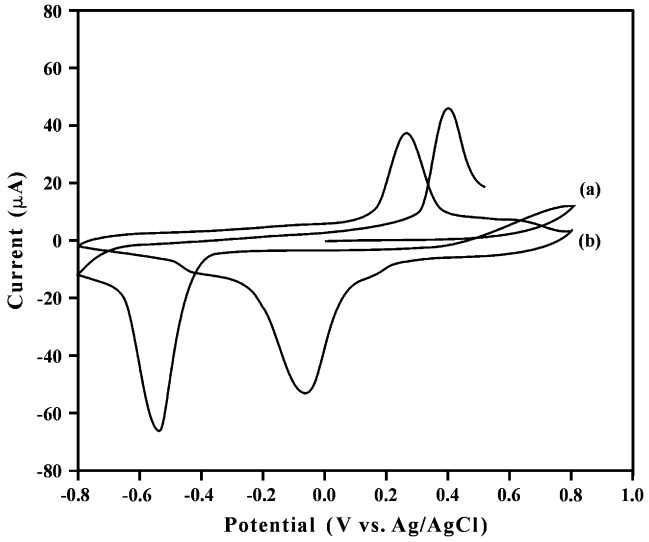

Fig. 6. Cyclic voltammogram of (a) monomer APOD and (b) undoped PAPOD film adhered on a platinum foil in 0.1 mol dm^{-3} $LiClO_4$/AN solution. Scan rate 10 mV s^{-1}.

Fig. 6b depicts the cyclic voltammogram of undoped PAPOD film performed under the identical condition to that of APOD. The redox behavior of PAPOD is similar to that of its monomer APOD. However, the oxidation and reduction potentials of PAPOD are more negative and positive, respectively, than those of APOD. Namely, the peak separation between the reduction and oxidation potential of the polymer (ca. 0.32 V) is narrower than that of its monomer (ca. 0.92 V). These results suggest that the cleavage (reduction process) of S–S bonds and the recombination (oxidation process) of thiolate anion in PAPOD are easier and more reversible than APOD. The great improvements of cleavage and recombination efficiency of S–S bonds may be attributed to the heavy electron donating characteristics of side-chain O–S–S–O bonds confined between the main chains of polyaniline. Also the fundamental reason is that S–S bonds in the polymer are confined between two polymer chains, and when one S–S bond is broken, it can be easily recombined since the two $-S^-$ groups cannot move away – they are chemically bonded to two large immobile neighbor chains.

The consecutive cyclic voltammograms of undoped PAPOD film adhered on platinum foil in an AN solution containing 0.1 mol dm^{-3} HCl and 0.1 mol dm^{-3} $LiClO_4$ are shown in Fig. 7. The potential was cycled 15 times between −0.6 and 0.8 V continuously with a scan rate of 10 mV s^{-1}. The peak current values of the redox peaks have been found to increase with number of cycles. A pair of redox peaks (ca. −0.06 and 0.26 V), corresponding to the redox reactions of the $2S^-/S–S$ couple, in the first cycle disappeared and developed into two pairs of redox peaks after several cycles. This cyclic voltammogram pattern is similar to that of the electrosynthesis process for HCl-doped PANi. So it is inferred that two oxidation peaks at ca. 0.17 and 0.48 V are attributed to deprotonated (doping) process, and two reduction peaks at ca. 0.03 and 0.42 V are attributed to the protonated (undoping) process

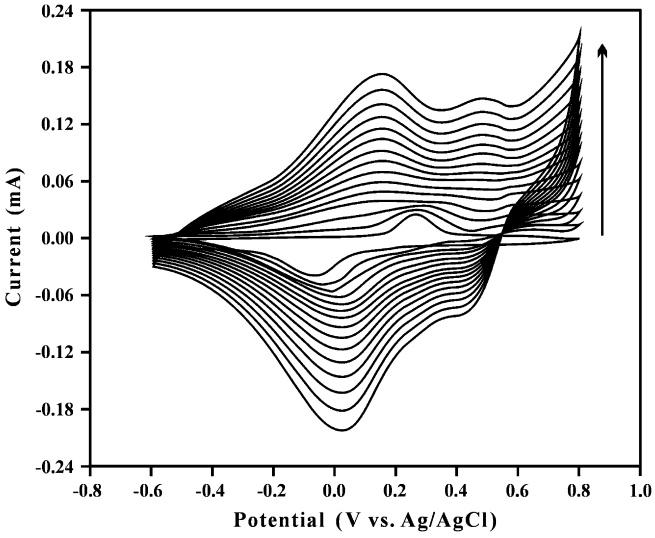

Fig. 7. The consecutive cyclic voltammograms of undoped PAPOD film adhered on a platinum foil in an AN solution containing 0.1 mol dm^{-3} HCl and 0.1 mol dm^{-3} $LiClO_4$. Scan rate 10 mV s^{-1}.

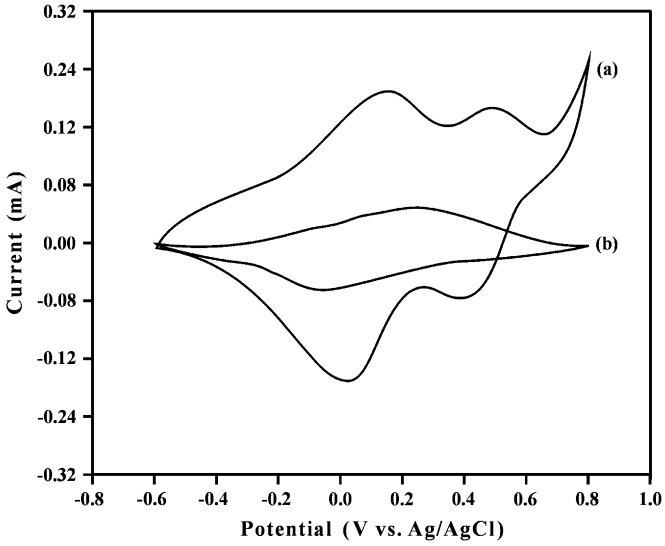

Fig. 8. Cyclic voltammograms of HCl-doped PAPOD film adhered on a platinum foil in an AN solution containing 0.1 mol dm^{-3} $LiClO_4$. (a) The first potential scan and (b) the 20th potential scan. Scan rate 10 mV s^{-1}.

of PAPOD. Moreover, the redox reaction of amine/imine groups has occurred at nearly the same range of potential as that of thiol or thiolate anion/disulfide groups in the same material. These results imply that the intramolecular self-electrocatalyzed effects have occurred between the conducting main-chain and the side chain of the disulfide bonds in PAPOD. This redox property as well as the better reversibility of PAPOD suggests that this new polyaniline derivative containing disulfide bonds can provide a comparatively high power density when it is used as a new energy-storage material.

For a further support of the assignment for the redox peaks of the main chain of conductive polyaniline and the side chain of disulfide bonds in PAPOD, we have recorded the consecutive cycle voltammograms of HCl-doped PAPOD in nonprotonic media (Fig. 8). The two pairs of redox peaks due to the protonic undoping–doping processes at first sweep have been observed. Owing to the irreversible deprotonated (undoping) processes, the peak current values have decreased with increasing number of cycles and the two pairs of redox peaks have been shrunk to one pair of wide redox peaks (ca. −0.06 and 0.25 V), which are in good agreement with the pair of redox peaks in Figs. 6b and 7. In the mean while, protonic undoping–doping processes have occurred at the same range of potential as that of thiolate anion/disulfide redox process.

3.2.3. Charge/discharge behavior

A novel redox system, PAPOD has been proposed as a high energy-storage material such as the cathode for high capacity lithium secondary batteries. The theoretical charge capacity of PAPOD cathode can be calculated as 261 mAh g^{-1}, assuming that $n = 2.8$ electron reactions per repeat unit has undergone in the reduction processes of main-chain polyaniline and side-chain S–S bonds. That is, (1) there are $n = 0.8$ electron transfer per repeat unit to occur when polyaniline chain of this polymer is oxidized to a conservative ca. 40% of the fully quinoid form according to the facts of XPS and FT-IR above [5]; (2) The S–S bond system of this polymer provides reversible $n = 2.0$ electron reactions accompanied by bond cleavage and recombination process per repeat unit.

The lithium battery was fabricated with the composite containing PAPOD (42 wt%), carbon (48 wt%) and binder (10 wt%) as the cathode, 1 mol dm^{-3} $LiClO_4$/PC–EC (1:1, by volume) as the electrolyte, and lithium as the anode. The charge/discharge test for the lithium battery was performed at a current density of 0.1 mA cm^{-2} with a termination voltage of 1.0 V. Fig. 9 shows the first discharge curve. The voltage drops from 3.7 to 2.2 V at initial stage of the discharge process. This phenomenon may be closely related to the internal resistance of the composite cathode, which is not mixed uniformly. The curve is very flat at 2.0 V, which suggests a single-step discharge process. This result indicates that the reduction

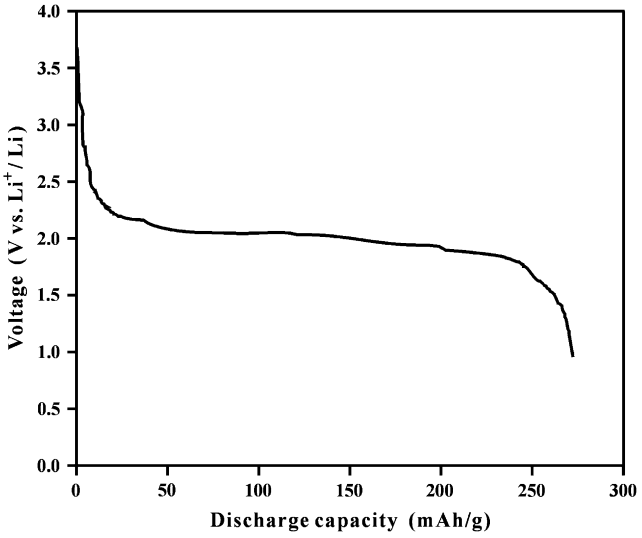

Fig. 9. The first discharge curve of the Li/PAPOD cell at the room temperature. Current density was 0.1 mA cm^{-2} and termination voltage was 1.0 V vs Li/Li^+.

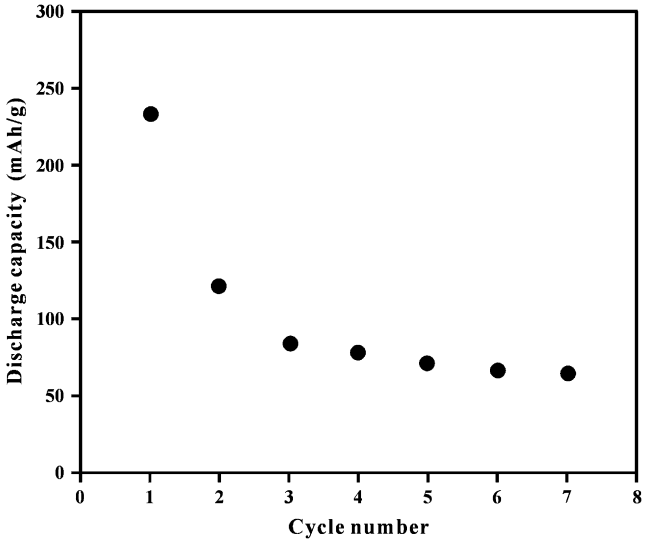

Fig. 10. Variation of discharge capacity for Li/PAPOD cell with cycle number. Current density was 0.1 mA cm^{-2} and voltage range was 3.7–1.0 V vs Li/Li^{+}.

processes of main-chain polyaniline and side-chain S–S bonds have occurred at the same potential. This result is in excellent agreement with that of the cyclic voltammograms discussed above.

The specific capacitance and energy density are calculated to be 230 Ah kg^{-1} and 460 Wh kg^{-1}, respectively, based on the polymer's equivalent weight. These data support an unambiguous fact that PAPOD undergoes nearly three electron reactions per repeat unit so that the specific charge density is nearly consistent with the theoretical charge density.

However, the capacity of the cell after second cycle has decreased greatly and the loss of capacity has increased with increasing number of the repeated charge/discharge cycles as shown in Fig. 10. The short-life of the charge/discharge test could be attributed to impurities or low polymerization degree. On the other hand, preparation method or configuration of cathode is one of the important points for a high performance cathode. Fan and Fedkiw [49] reported that the cell with the casted cathode possessing high ohmic resistance could not be cycled and the cell with the high pressure compacted cathode showed good cycling performance under high rate discharge. Further optimization for preparation of PAPOD composite cathode, such as preparation condition, mixing ratio, etc. should be improved for construction of a high performance battery.

4. Conclusion

A novel conductive polyaniline derivative as a new energy-storage material has been synthesized by moderate oxidant ferric chloride in an acidic medium. XPS, UV–vis spectroscopy, FT-IR, FT-Raman, and elemental analysis data suggest that the expected decrease in the doping level and in the conjugation degree of PAPOD, in contrast with polyaniline, results from the steric hindrance and cross-linking structure of side-chain –O–S–S–O– groups in it. The electrical conductivity of this polymer (6.4×10^{-2} S cm^{-1}) is 2–3 orders of magnitude lower than that of HCl-doped polyaniline, but rather high than that of conventional organodisulfur compounds which exhibit no electrical conductivity. This conducting organodisulfide polymer is of great advantage for its application in the energy-storage material such a cathode of lithium battery.

The comparative cyclic voltammograms of monomer APOD, undoped PAPOD, HCl-doped PAPOD in neutral or acidic media indicate that the cleavage (reduction) and formation (oxidation) reaction of the S–S bonds in PAPOD are more facile and reversible than those of its monomer, and the redox reaction (doping/undoping processes) of the main-chain π-conjugated system occurs in the same potential range as that of the side-chain thiol (or thiolate anion)/disulfide in this polymer. These facts signify that the intramolecular self-catalyzed effects occur between the main-chain conductive polyaniline and the side-chain disulfide bonds in PAPOD.

The discharge test of Li/PAPOD cell shows a flat curve at 2.0 V with a discharge capacity of 230 mAh g^{-1}-polymer and an energy density of 460 mWh g^{-1}-polymer, which is about 2–3 times higher than those of inorganic intercalation compounds. Such higher capacity is realized at the same potential by both S–S/–S and anilinium/aniline reductive reaction in PAPOD. However, the poor performance of its charge/discharge cycle will be improved by further investigation.

Acknowledgements

This research was funded by National (50673022) and Guangdong Province (020602) Science Foundation of China, and Science and Technology Project of Guangdong Province (2003C105002) and Guangzhou City (2004J1-C0121) of China.

References

[1] Visco SJ, Mailhe CC, De Honghe LC, Armand MB. J Electrochem Soc 1989;136:661–4.
[2] Doeff MM, Visco SJ, De Jonghe LC. J Appl Electrochem 1992;22:307–9.
[3] Naoi K, Menda M, Ooike H, Oyama N. J Electroanal Chem 1991;318:395–8.
[4] Oyama N, Tatsuma T, Sato T, Sotomura T. Nature (London) 1995;373:598–600.
[5] Oyama N, Pope JM, Sotomura T. J Electrochem Soc 1997;144:L47–51.
[6] John MP, Oyama N. J Electrochem Soc 1998;145:1893–901.
[7] Wang B. J Electrochem Soc 2002;149:A1171–4.
[8] Inamasu T, Yoshitoku D, Sumi-otorii Y, Tani H, Ono N. J Electrochem Soc 2003;150:A128–32.
[9] Tsutsumi H, Fujita K. Electrochim Acta 1995;40:879–82.
[10] Tsutsumi H, Okada K, Fujita K, Oishi T. J Power Sources 1997;68:735–8.
[11] Giffard M, Nguyen TP, Molinie P, Lefrant S. Synth Met 1999;101:453–4.
[12] Wen TC, Huang LM, Gopalan A. J Electrochem Soc 2001;148:D9–17.
[13] Wen TC, Yang CH, Chen YC, Lin WC. J Electrochem Soc 2003;150:D123–8.
[14] Tsutsumi H, Oyari Y, Onimura K, Oishi T. J Power Sources 2001;92:228–33.
[15] Naoi K, Kawase K, Mori M, Komiyama M. J Electrochem Soc 1997;144:L173–5.

[16] Diaz FR, Sanchez CO, del Valle MA, Radic D, Bernede JC, Tregouet Y, et al. Synth Met 2000;110:71–7.
[17] Uemachi H, Iwasa Y, Mitani T. Electrochim Acta 2001;46:2305–12.
[18] Su YZ, Gong KC. Chem J Chin Univ 2001;22:479–81.
[19] Naoi K, Suematsu S, Komiyama M, Ogihara N. Electrochim Acta 2002; 47:1091–6.
[20] Su YZ, Niu YP, Xiao YZ, Xiao M, Liang ZX, Gong KC. J Polym Sci Polym Chem Ed 2004;42:2329–39.
[21] Vijayakrishna K, Sundararajan G. Polymer 2006;47:3363–71.
[22] Zhang W, Shiotsuki M, Masuda T. Polymer 2006;47:2956–61.
[23] Yu TL, Wu CC, Chen CC, Huang BH, Wu JC, Lin CC. Polymer 2005; 46:5909–17.
[24] Ginderu JM, Richter AF, MacDiarmid AG, Epstein A. J Solid State Commun 1987;63:97–101.
[25] Diaz FR, Sanchez CO, del Valle MA, Tagle LH, Bernede JC, Tregouet Y. Synth Met 1998;92:99–106.
[26] Jens K, Burçak A, Walter K. Polymer 2006;47:3302–14.
[27] Quijada R, Guevara JL, Galland GB, Rabagliati FM, Lopez-Majada JM. Polymer 2005;46:1567–74.
[28] Chan HSO, Ng SC, Sim WS, Tan KL, Tan BTG. Macromolecules 1992; 25:6029–34.
[29] Chen SA, Hwang GW. J Am Chem Soc 1995;117:10055–62.
[30] Chan HSO, Ho PKH, Ng SC, Tan BTG, Tan KL. J Am Chem Soc 1995; 117:8517–23.
[31] Yue J, Epstein AJ. Macromolecules 1991;24:4441–5.
[32] Tan KL, Tan BTG, Kang ET, Neoh KG. Phys Rev B 1989;39: 8070–3.
[33] Chan HSO, Ho PKH, Tan KL, Tan BTG. Synth Met 1990;35:333–44.
[34] Kumar SN, Gaillard F, Bouyssoux G. Synth Met 1990;36:111–27.
[35] Eular WB. Solid State Commun 1986;57:857–9.
[36] Stafstrom S, Bredas JL, Epstein AJ, Woo HS, Tanner DB, Huang WS, et al. Phys Rev Lett 1987;59:1464–7.
[37] Asturias GE, MacDiarmid AG, McCall RP, Epstein AJ. Synth Met 1989;29:E157–9.
[38] Masters JG, Sun Y, MacDiarmid AG, Epstein AJ. Synth Met 1991;41: 715–8.
[39] Cataldo F, Maltese P. Polym Adv Technol 2001;12:293–9.
[40] Wan M. J Polym Sci Polym Chem Ed 1992;30:543–9.
[41] Chan HSO, Ng SC, Ho PKH. Macromolecules 1994;27:2159–64.
[42] Glarum SH, Marshall JH. J Phys Chem 1988;92:4210–7.
[43] Yue J, Wang ZF, Cromack KR, Epstein AJ, MacDiarmid AG. J Am Chem Soc 1991;113:2665–71.
[44] Lux F. Polymer 1994;35:2915–36.
[45] Cataldo F. Eur Polym J 1996;32:43–50.
[46] DeArmitt C, Armes SP, Winter J, Uribed FA, Gottesfeid S, Mombourquette C. Polymer 1993;34:158–62.
[47] Cataldo F, Maltese P. Eur Polym J 2002;38:1791–803.
[48] Wang ZH, Epstein AJ, Ray A, MacDiarmid AG. Synth Met 1991;41: 749–52.
[49] Fan J, Fedkiw PS. J Power Source 1998;72:165–73.